CHEMBIOCHEM

DOI: 10.1002/cbic.200700489

Zinc(II) Coordination Complexes as Membrane-Active Fluorescent Probes and Antibiotics

Kristy M. DiVittorio,[a] W. Matthew Leevy,[a, b] Edward J. O'Neil,[a] James R. Johnson,[a] Sergei Vakulenko,[a] Joshua D. Morris,[a] Kristine D. Rosek,[a] Nathan Serazin,[a] Sarah Hilkert,[a] Scott Hurley,[a] Manuel Marquez,[c, d, e] and Bradley D. Smith*[a]

Molecular probes with zinc(II)-(2,2′-dipicolylamine) coordination complexes associate with oxyanions in aqueous solution and target biomembranes that contain anionic phospholipids. This study examines a new series of coordination complexes with 2,6-bis(zinc(II)-dipicolylamine)phenoxide as the molecular recognition unit. Two lipophilic analogues are observed to partition into the membranes of zwitterionic and anionic vesicles and induce the transport of phospholipids and hydrophilic anions (carboxyfluorescein). These lipophilic zinc complexes are moderately toxic to mammalian cells. A more hydrophilic analogue does not exhibit mammalian cell toxicity ($LD_{50} > 50\,\mu g\,mL^{-1}$), but it is highly active against the Gram-positive bacteria Staphylococcus aureus *(MIC of $1\,\mu g\,mL^{-1}$). Furthermore, it is active against clinically important* S. aureus *strains that are resistant to various antibiotics, including vancomycin and oxacillin. The antibiotic action is attributed to its ability to depolarize the bacterial cell membrane. The intense bacterial staining that was exhibited by a fluorescent conjugate suggests that this family of zinc coordination complexes can be used as molecular probes for the detection and imaging of bacteria.*

Introduction

Molecules with selective cell surface recognition properties are used extensively in cell biology, biotechnology, and medicine.[1] For example, high-molecular-weight antibodies are employed as reagents for purification processes, sensing assays, and imaging technologies.[2] They also have value as pharmaceutical agents.[3] Various small biomolecules, especially peptides, are known to exhibit selective cell-targeting properties.[4] In addition, small molecules that target and disrupt the membranes of microorganisms are pursued as drug candidates for treating various infectious diseases.[5] As part of a program to develop molecular probes for the imaging of infectious disease, we are investigating synthetic molecules that can differentiate between healthy mammalian cells and microorganisms.[6] The cell plasma membrane is a complicated supramolecular assembly of proteins and polar lipids, and there is a rich array of potential biomarkers for targeting. However, a notable difference between these two types of cells is the composition and charge of the polar lipids that decorate the cell surface. The plasma membrane outer leaflet of most mammalian cells is primarily composed of zwitterionic phospholipids such as sphingomyelin and phosphatidylcholine.[7] In contrast, the exterior surface of bacterial cells contains a high fraction of anionic phospholipids and related anionic amphiphiles.[8] This difference in surface charge helps explain why cationic compounds have an inherent selectivity for bacterial cells over mammalian cells. Indeed, most classes of antimicrobial peptides have a net positive charge.[9]

This study focuses on the cell recognition properties of synthetic zinc coordination complexes.[10] These compounds have been examined extensively as simplified models for various phosphate-binding processes, and also as functional molecules such as catalysts, sensors, and receptor antagonists.[11] Recently, we discovered that fluorescent coordination complexes **1**, which has two zinc(II) 2,2′-dipicolylamine units have a remarkable ability to selectively stain bacterial cells in preference to mammalian cells.[12] Furthermore, we have developed fluorescent near-infrared derivatives of **1** that can target and identify bacterial infection in mice.[13] Here, we describe the cell recognition properties of a second-generation design, **2**, which is based on 2,6-bis(zinc(II)-dipicolylamine)phenoxide as a synthetic anion-binding receptor. This dinuclear zinc coordination complex associates strongly with phosphate derivatives in aqueous solution and to a lesser extent with carboxylates (Scheme 1).[14] We have previously reported the tyrosine deriva-

[a] *K. M. DiVittorio, Dr. W. M. Leevy, E. J. O'Neil, J. R. Johnson, Dr. S. Vakulenko, J. D. Morris, K. D. Rosek, N. Serazin, S. Hilkert, S. Hurley, Prof. Dr. B. D. Smith*
Department of Chemistry and Biochemistry, University of Notre Dame
251 Nieuwland Science Hall, Notre Dame, IN 46556 (USA)
Fax: (+1) 574-631-6652
E-mail: smith.115@nd.edu

[b] *Dr. W. M. Leevy*
Current address: INEST (Interdisciplinary Network of Emerging Science and Technologies) Group Postgraduate Program
Research Center, Philip Morris USA
4201 Commerce Road, Richmond, VA 23234 (USA)

[c] *Dr. M. Marquez*
NIST Center for Theoretical and Computational Nanosciences
Gaithersburg, MD 20899 (USA)

[d] *Dr. M. Marquez*
Harrington Department of Bioengineering, Arizona State University
Tempe, AZ 85287 (USA)

[e] *Dr. M. Marquez*
Research Center, Philip Morris USA
4201 Commerce Road, Richmond, VA 23234 (USA)

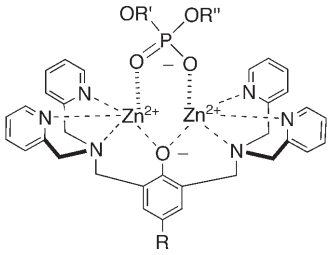

Scheme 1. Association of zinc complex **2** with a phosphate anion.

tive **4**, and have briefly described its vesicle-binding properties.[15] The ease of synthetic manipulation makes **4** a versatile building block for conjugation.[16] The fluorescent conjugate **7** has negligible affinity for vesicle membranes that are composed only of zwitterionic phosphatidylcholine, but it associates strongly with vesicles that include anionic phospholipids and even penetrates into the bilayer membrane. We now describe in detail the vesicle and cell membrane recognition properties of this family of zinc coordination complexes. We find that lipophilic analogues **5** and **6** are able to partition into zwitterionic vesicles and promote the translocation of phospholipids and hydrophilic anions across the vesicle membrane.

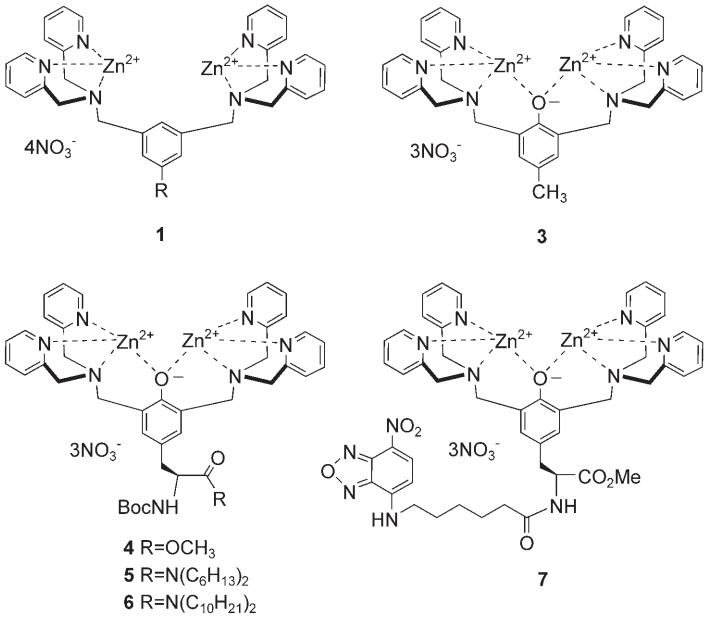

4 R=OCH_3
5 R=$N(C_6H_{13})_2$
6 R=$N(C_{10}H_{21})_2$

Furthermore, **5** and **6** are moderately toxic to mammalian cells. The more hydrophilic version, **3** does not interact with mammalian cells but it exhibits potent and selective toxicity against the pathogenic bacterium *Staphylococcus aureus*. Mechanistic studies suggest that **3** depolarizes the bacterial membrane, which explains why it is highly active against strains of *S. aureus* that are resistant to the important clinical drugs vancomycin and oxacillin.

Results and Discussion

Vesicle Studies

Enhanced phospholipid flip-flop: The ability of zinc complexes **3**–**6** to associate with vesicle membranes and promote inward phospholipid translocation (Scheme 2) was measured by using

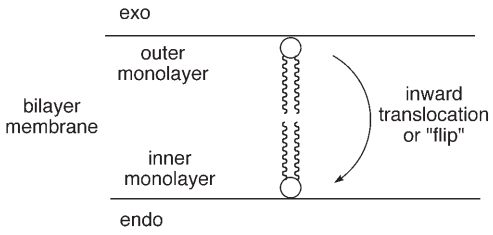

Scheme 2. Phospholipid translocation.

fluorescent 7-nitrobenz-2-oxa-1,3-diazol-4-yl (NBD)-phospholipids and an established NBD-dithionite quenching assay.[17] The method is based on the ability of dithionite to chemically react with the NBD-chromophore to give a non-fluorescent product. Because the dithionite anion diffuses very slowly through vesicle membranes, it will only react and quench the fluorescence of an NBD-phospholipid in the outer monolayer of the membrane. The background translocation experiment starts by adding a small amount of NBD-phospholipid (0.5% of total lipid) to a dispersion of vesicles. The NBD-phospholipid incorporates into the outer monolayer to create 100% exo-labeled vesicles. Every 15 minutes, an aliquot of vesicles is removed and treated with dithionite, which allows the percent of exo NBD-phospholipid to be determined. The experiment progresses towards an equilibrated value of about 60% exo NBD-phospholipid. The half-life is the time to reach 80% exo NBD-phospholipid, and the unassisted background value is many hours.

The structures of the probes and phospholipids are provided in Scheme 3 and the translocation half-lives that are induced by the presence of compounds **3**–**6** are given in Table 1. These experiments use two NBD-phospholipid probes (zwitterionic NBD-PC and anionic NBD-PG) with two types of vesicle systems

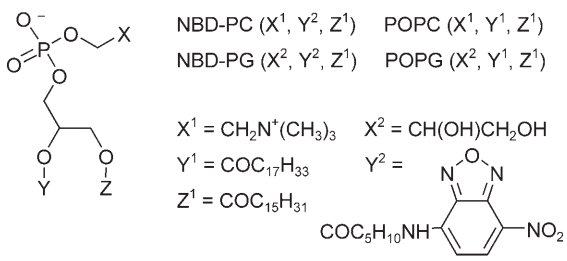

Scheme 3. Probes and phospholipids.

Table 1. Effect of zinc complexes on membrane translocation half-lives.

	Probe translocation half-life [min][a]		
	Vesicles: 100% POPC		Vesicles: POPG/POPC(1:9)
Complex (1 μM)	NBD-PG	NBD-PC	NBD-PG
3	>60	>60	30
4	>60	>60	20
5	12	>60	20
6	20	>60	>60

[a] Time to reach 80% exo NBD-phospholipid, average half-life error ±33%.

(zwitterionic vesicles composed of 100 mol% POPC, and anionic vesicles composed of POPG/POPC, 1:9). To induce translocation of an NBD-phospholipid probe, the zinc complex must penetrate the vesicle membrane and also associate with the probe to make a charge-neutral aggregate that can diffuse across the membrane. Because all of the zinc complexes are cationic, it is not surprising that they do not promote the translocation of zwitterionic probe, NBD-PC (translocation half-life >60 min) in any vesicle system. The relatively hydrophilic complexes **3** and **4** do not accelerate flip-flop of the anionic NBD-PG probe in POPC vesicles, presumably because these hydrophilic zinc complexes do not associate with the nearly neutral vesicles (the anionic probe is only present at 0.5% of total lipid). However, **3** and **4** do associate with anionic POPG/POPC (1:9) vesicles and shorten the translocation half-life of NBD-PG probe to 30 and 20 min, respectively. In contrast to this vesicle selectivity, the more lipophilic zinc complexes **5** and **6** partition into both the uncharged and anionic vesicle systems and strongly promote NBD-PG flip-flop. Literature evidence suggests that the anionic phosphate diester head group of the PG probe is chelated to both zinc cations (Scheme 1),[14] and the aggregate diffuses across the bilayer membrane. Because each of these zinc complexes has a net +3 charge, the requirement for charge balance requires the simultaneous transport of several anions across the membrane.[18]

Enhanced carboxyfluorescein transport: The carboxyfluorescein (CF) leakage assay was employed to determine if the zinc complexes could transport hydrophilic anions across vesicle membranes.[19] CF was encapsulated inside vesicles under high, self-quenching concentrations. Transport out of the vesicles leads to dilution of the dye and a large increase in fluorescence intensity. In agreement with the phospholipid translocation data, the hydrophilic zinc complexes **3** and **4** did not induce CF leakage from zwitterionic POPC vesicles and produced only slight leakage from anionic POPG/POPC, 1:9 vesicles (data not shown). The more lipophilic zinc complexes **5** and **6** were much more effective at promoting CF leakage. Shown in Figure 1 is the leakage that is induced upon addition of complex **6**. The data highlight two trends, 1) almost twice as much leakage occurs from zwitterionic, POPC vesicles than from anionic POPG/POPC, 1:9 vesicles, and 2) CF leakage is completely inhibited when the external vesicle solution is changed from 5 mM TES in 100 mM NaCl, to 5 mM TES in 75 mM Na_2SO_4. These two results are consistent with a membrane transport process that involves direct coordination of the CF to the zinc complex. Thus, CF leakage from the anionic, POPG/POPC vesicles is inhibited because the anionic POPG head group competes for the zinc coordination sites (Scheme 1). Similarly, CF release from the vesicles can only occur if there is concomitant entry of a counter anion, which is kinetically feasible when the external solution contains the relatively lipophilic chloride, but it becomes very unfavorable when the external solution only contains sulfate dianion. The sulfate dianion is extremely hydrophilic, and its transport into a membrane involves a major dehydration penalty. Sulfate-inhibited transport is a signature of anion counter-transport processes that involve intimate association between the anion and the transporter.[20]

Proof that the zinc cations are critical for membrane transport was obtained by measuring CF transport activity in the presence and absence of zinc cations. As shown in Figure 2, addition of 1 μM of apo-**6** (i.e., the uncharged phenol version of **6** without the two zinc cations) at 50 s to vesicles that contain CF does not produce CF leakage. However, if two molar

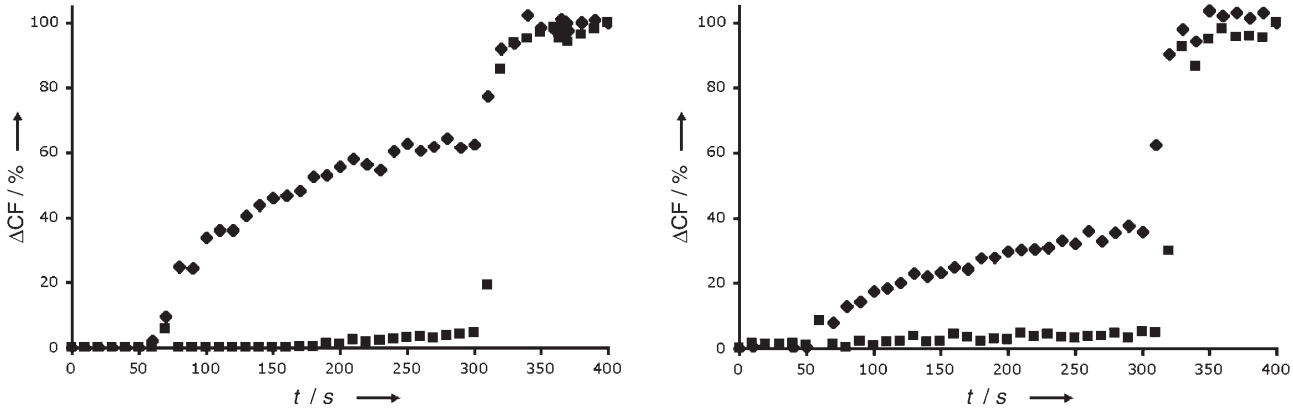

Figure 1. CF transport from vesicles that was induced by the addition of zinc complex **6** (1 μM) at 50 s to vesicles in 5 mM TES (pH 7.4) buffer with either 100 mM NaCl (◆) or 75 mM Na_2SO_4 (■), followed by vesicle lysis with Triton X-100 at 300 s. Left: zwitterionic vesicles composed of POPC; right: anionic vesicles composed of POPG/POPC (1:9). In the *y*-axis, ΔCF is the amount of CF that was released from the vesicles.

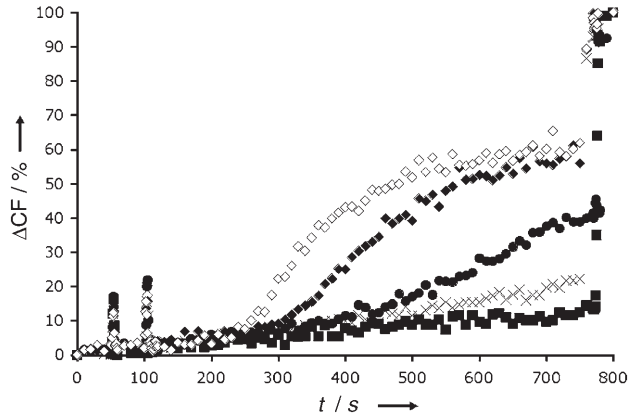

Figure 2. Dependence of CF release on zinc complexation to form transport active **6**. Apo-**6** (1 μM) was added at 50 s to POPC vesicles (25 μM). Inside the vesicles is 5 mM TES, 50 mM CF, 100 mM NaCl (pH 7.4) buffer; outside the vesicles is 5 mM TES, 100 mM NaCl (pH 7.4) buffer. $Zn(NO_3)_2$ (0 μM (■), 0.25 μM (×), 0.5 μM (●), 1 μM (◆) and 2 μM (◇)) was added at 100 s and the vesicles were lysed with Triton X-100 at 750 s. In the y-axis, ΔCF is the amount of CF that was released from the vesicles.

equivalents of $Zn(NO_3)_2$ are subsequently added to the vesicle dispersion at 100 s, extensive CF leakage begins to occur after a 150 s induction period, which is presumably the time period that is required to form the dinuclear zinc complex **6**. The final amount of CF leakage is essentially the same as that observed when the same concentration of preformed zinc complex **6** (1 μM) is added to the vesicles (compare Figure 2 with Figure 1). The other leakage curves in Figure 2 show that the amount of transport is decreased and the induction time is increased with sub-stoichiometric amounts of added $Zn(NO_3)_2$. These features are additional evidence that a multicomponent association process is required to produce **6** as the kinetically active CF transporter. Finally, the dependence of CF transport was measured at different concentrations of preformed **6**. As shown in Figure 3, the initial flux is directly proportional to the concentration of **6**, which suggests that CF transport is produced by a stoichiometric recognition process and is not simply due to nonspecific membrane disruption. Taken together, the CF leakage data present a compelling kinetic case that a liphophilic dinuclear zinc complex is required for CF transport across uncharged POPC vesicles, and that transport likely involves direct coordination of the oxyanion to the two zinc cations.

The vesicles studies raise the following hypothesis. Lipophilic zinc complexes **5** and **6** can partition into mammalian and bacterial cell membranes and exhibit general cell toxicity by promoting anion transport and phospholipid flip-flop. In contrast, hydrophilic analogues **3** and **4** do not associate with the zwitterionic surfaces of mammalian cells, but they can partition into the anionic membranes of bacterial cells, and thus exhibit selective cell toxicity. The following cell toxicity studies were conducted to confirm this hypothesis.

Mammalian cell toxicity

Compounds **3**–**6** were evaluated for toxicity against three human cancer cell lines; Jurkat (T-cell leukemia), PC3 (androgen-independent prostatic) and LNCaP (androgen-dependent prostatic) cells. The colorimetric MTT assay was used to determine cellular viability. Briefly, the cells were dispersed in 96-well plates and incubated at 37 °C for 24 h. The growth media was exchanged with fresh media and then treated with MTT [3-(4,5-dimethylthiazol-2-yl)-2,5-diphenyltetrazolium bromide]. In healthy cells, with active mitochondrial systems, the MTT is reduced to formazan, a purple compound. The amount of formazan absorption is related to the number of viable cells. The toxicity of the zinc complexes was observed to be dose dependent, and the LD_{50} values are listed Table 2. The hydrophilic zinc complexes **3** and **4** did not cause significant cell death at concentrations up to 50 μM. However, there was moderate toxicity with the more lipophilic complexes, **5** and **6** (LD_{50} values between 2 and 30 μM), a trend that correlates with membrane transport activity. Thus, it appears that mammalian cell toxicity increases with cell permeability of the zinc complex. While the precise cell death mechanism is not clear at present, it is relevant to note that a structurally related series of cell permeable

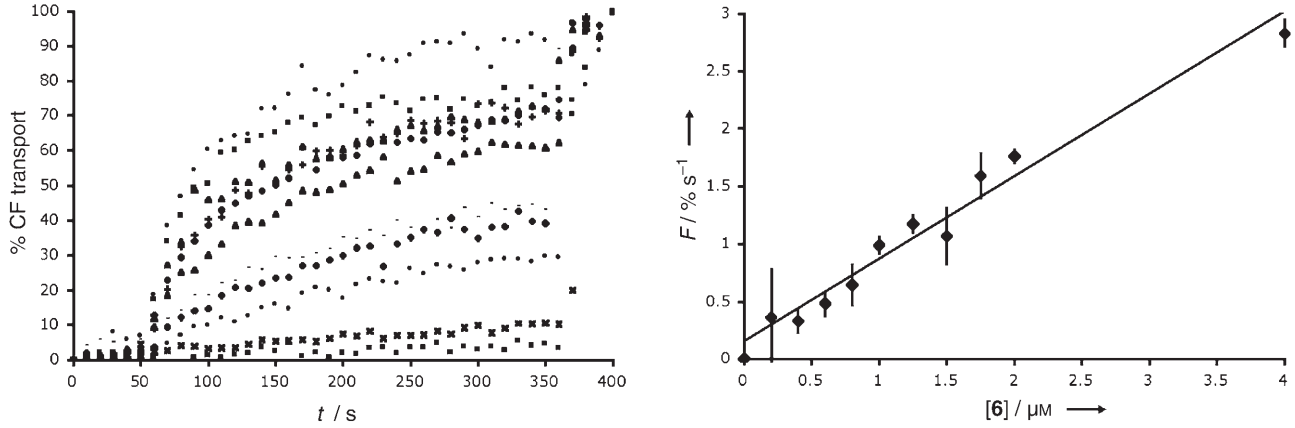

Figure 3. Initial CF flux (*F*) at different concentrations of **6**. Vesicles [25 μM lipid, POPC/cholesterol (7:3), encapsulating 5 mM TES, 100 mM NaCl, 50 mM CF (pH 7.4) buffer] were dispersed in 5 mM TES, 100 mM NaCl (pH 7.4) buffer and treated with varying concentrations of **6**. The initial flux is the %CF transport at 20 s after addition of **6**. The error bars reflect the averages of three independent experiments. In the *y*-axis, *F* is the amount of CF released from the vesicles.

Table 2. Mammalian cell toxicity.

Zinc Complex	LD_{50} [μM][a] Jurkat cells	PC3 cells	LNCaP cells
3	>50	>50	>50
4	>50	>50	>50
5	30	5	20
6	5	2	5

[a] Concentration of zinc complex required to decrease cell viability to 50%.

zinc complexes was very recently shown to induce apoptosis by repression of bcl-2 expression.[21]

Bacteria cell imaging and toxicity

The ready availability of NBD-conjugate **7** allowed us to conduct bacterial cell imaging by using fluorescence microscopy. Figure 4 shows fluorescence images of *Escherichia coli* and

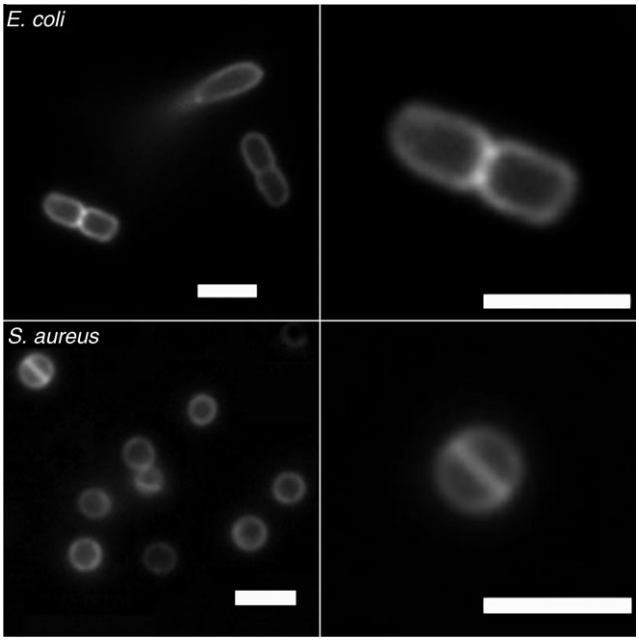

Figure 4. Fluorescence micrographs of *E. coli* (top) and *S. aureus* (bottom) cells, after treatment with zinc complex **7**. The right panels are magnified to show single cells undergoing binary fission. Scale bar in each image represents 2 μm.

S. aureus that have been treated with 10 μM of **7**, and subsequently washed twice with buffer. In both cases, the staining is localized to the cell walls, in agreement with previous imaging results that were obtained with fluorescent probes that were based on structure **1**.[12] Also shown in Figure 4 are magnified examples of staining patterns that are consistent with cells that are undergoing the process of binary fission. Gram-positive bacteria like *S. aureus* are known to form an equatorial membrane that divides the cell into hemispheres before replication.[22] Meanwhile, Gram-negative bacteria like *E. coli* replicate by a symmetric invagination at the equator, which "pinches" the cell in half.[23] The NBD fluorophore is susceptible to photobleaching, which limits its utility in fluorescence microscopy. However, the intense staining that was exhibited by **7** is proof of concept that fluorescent conjugates of this family of zinc complexes should be useful additions to the small group of synthetic fluorescent probes that can target bacteria.[24]

Because the hydrophilic zinc complex **3** was not toxic to mammalian cells, we evaluated its antibacterial activity against *S. aureus* and *E. coli* by using the minimum inhibitory concentration (MIC) method.[25] The growth of *E. coli* was not prevented by the presence of **3** at the highest tested concentration of 100 $\mu g\,mL^{-1}$. However, *S. aureus* (ATCC 29213) cells were remarkably susceptible, and exhibited a MIC value of 1 $\mu g\,mL^{-1}$, which corresponds to a therapeutic index that is >50-fold selective for *S. aureus* over mammalian cells. This potent antibiotic activity contrasts with the low toxicity that is exhibited by 4-cresol (>100 $\mu g\,mL^{-1}$ to inhibit *S. aureus* growth),[26] and the first-generation zinc complexes that were based on **1** (weakly toxic against *E. coli* or *S. aureus*). Bacterial growth inhibition assays were also conducted against two drug-resistant strains of *S. aureus*. As listed in Table 3, the same MIC of 1 $\mu g\,mL^{-1}$ was obtained against: 1) *S. aureus* (NRS100), a strain that is resistant to β-lactam antibiotics, including the drug oxacillin, and 2) *S. aureus* (VRS1), which has resistance to both vancomycin and oxacillin. Additional experiments were performed to determine if zinc complex **3** can act in synergy with known antibiotics; however, sub-lethal concentrations of **3** did not significantly affect the activity of vancomycin or oxacillin.

Table 3. Minimum inhibitory concentration (MIC).

Microorganism	Antibiotic MIC [$\mu g\,mL^{-1}$][a] **3**	Van[b]	Oxa[c]	0.1 $\mu g\,mL^{-1}$ **3** + Van	0.1 $\mu g\,mL^{-1}$ **3** + Oxa
S. aureus 29213	1	1	0.3	1	0.1
S. aureus (NRS 100)	1	2	256	2	256
S. aureus VRS1 (NARSA)	1	1000	256	1000	256

[a] Minimum inhibitory concentration. [b] Vancomycin. [c] Oxacillin.

Evidence that metal coordination is necessary for antibiotic activity is found in the large difference in MIC values for the uncomplexed apo-**3** and it isomer apo-**8**. Against *S. aureus*, the MIC values were 1 $\mu g\,mL^{-1}$ for apo-**3** and >40 $\mu g\,mL^{-1}$ for apo-**8**. Because apo-**8** has two 3,3′-picolylamine units, it cannot form stable metal-coordination complexes, and it exhibits a high MIC value, which is typical for a simple phenol.[26] In contrast, there is little doubt that apo-**3** is rapidly converted into a metal complex as seen in the vesicle studies (Figure 2). Because the concentration of zinc(II) in the testing media was around 15 μM,[27] the formation of zinc complex **3** is highly favored, however, we cannot rule out the possibility that other metal complexes might also be formed, especially copper(II) complexes. Even if these other metal complexes are formed,

they are likely to have similar oxyanion recognition properties.[28]

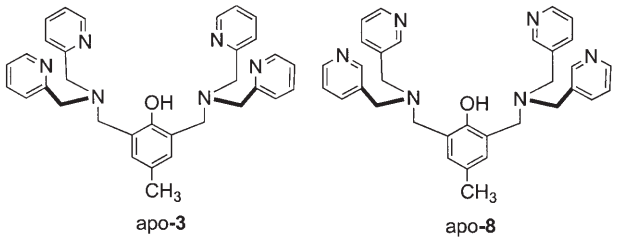

The vesicle studies and the bacteria imaging suggest that the antibiotic activity of **3** is due to its ability to selectively associate with the surface of the Gram-positive bacteria and possibly disrupt membrane function. Therefore, **3** was tested for its ability to depolarize the *S. aureus* membrane. An established assay was employed by using $DiSC_3(5)$, a fluorescent dye that is sensitive to membrane potential.[29] Healthy bacterial cells have an inside negative membrane potential due to potassium efflux through leakage channels, as well as active proton efflux. The cationic dye $DiSC_3(5)$ inserts into the membranes of these healthy cells, where it is concentrated and becomes self-quenched. Upon membrane depolarization, the dye is released into the extracellular solution and exhibits a marked increase in fluorescence intensity. The experimental data are provided in Figure 5. *S. aureus* cells (OD is 0.05) were suspended in a

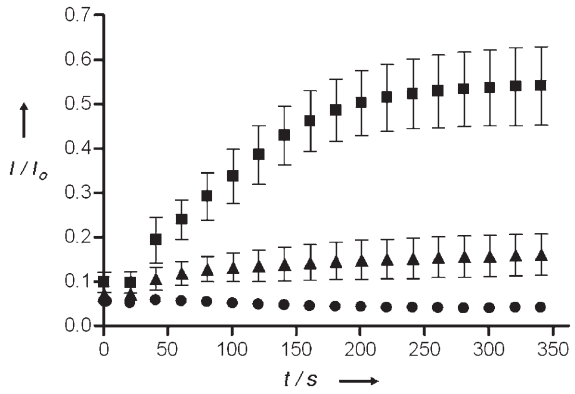

Figure 5. Membrane depolarization of *S. aureus* cells that was induced by **3** at 10 μg mL^{-1} (■), 1 μg mL^{-1} (▲), and buffer control (●).

salt-free buffer with $DiSC_3(5)$. Sodium chloride (60 mM final) was added to the extracellular solution, followed by **3** (10 or 1 μg mL^{-1}). Sodium chloride itself does not affect the cells because it has essentially no permeability at the resting state of healthy bacteria. However, the addition of **3** (10 μg mL^{-1}) caused a rapid increase in fluorescence intensity of the dye. At a MIC concentration of 1 μg mL^{-1}, the $DiSC_3(5)$ fluorescence increase is smaller, but is still above background. Because zinc complex **3** is only weakly amphiphilic, it is remarkable that it can depolarize bacterial membranes at such a low concentration. It is presently not clear how the membrane disruption occurs at the molecular level. However, we note that **3** is a densely charged, cationic molecule that targets the anionic phospholipid head groups in the bacterial membrane, a process that produces large fluctuations in local charge. Recently, high-level molecular dynamics simulations of bilayer membranes have led to the proposal of a field-induced pore model.[30] The simulations suggest that a localized charge imbalance, which would occur when several copies of **3** associate to a patch of bacterial membrane, can create a transmembrane electric field, which induces a transient water pore, and as a consequence ion transport and membrane depolarization.

Although **3** is inactive against *E. coli*, it is still a promising antibiotic lead because it is easy to produce and highly active against *S. aureus*, a significant human pathogen that is responsible for many common nosocomial infections. Indeed, **3** might be a cheap alternative to vancomycin for treating clinical oxacillin/methicillin-resistant *S. aureus* (MRSA) infections.[31] Furthermore, it is very hard for bacteria to become highly resistant against membrane-active antibiotics. For example, *S. aureus* resistance to the membrane active biocide, Triclosan, which is employed extensively in many consumer products, only increases MICs to the range of 2–4 μg mL^{-1}.[32]

Conclusions

As shown in Scheme 1, the dinuclear zinc complex **2** is a synthetic anion receptor that associates strongly with phosphate and to a lesser extent to carboxylate anions in aqueous solution. The lipophilic analogues **5** and **6** are able to partition into the membranes of zwitterionic and anionic vesicles and induce the transport of phospholipids and hydrophilic anions (carboxyfluorescein). These lipophilic zinc complexes are moderately toxic to mammalian cells, and thus they are unlikely to be useful as cell-selective antibiotic drugs. However, the more hydrophilic zinc complex **3** selectively associates with anionic membranes. As a result, it does not exhibit mammalian cell toxicity, but it is highly active against the Gram-positive bacterium *S. aureus*, including clinically important strains that are resistant to the antibiotics vancomycin and oxacillin. The antibiotic action of **3** appears to be due to its ability to depolarize the bacterial cell membrane. The impressive bacterial staining ability of fluorescent conjugate **7** suggests that this family of zinc coordination complexes might be very useful as cell-targeting probes for the detection and imaging of bacteria.

Experimental Section

Synthesis: The preparation of zinc complexes **3**, **4**, and **7** has been described previously.[14a,15,33] Zinc complexes **5** and **6** were prepared from the carboxylic acid form of the tyrosine derivative apo-**4**-CO_2H by using the following procedures.

Apo-4-CO_2H. A solution of **4** (1.0 g, 1.4 mmol), methanol (25 mL), and an equal volume of aqueous 1 M NaOH solution was stirred for 2 h at room temperature, neutralized with 2 M HCl, and extracted into chloroform. The chloroform extracts were washed three times with an equal volume of water and brine. The combined organic

layer was dried with Na_2SO_4 and evaporated to leave apo-**4**-CO_2H (0.83 g, 85% yield) which was used without further purification.

Zinc complex 5. A solution of apo-**4**-COOH (500 mg, 0.71 mmol) in anhydrous DMF (25 mL) was treated with *N,N'*-dihexylamine (158 mg, 0.85 mmol), 1-ethyl-3-(3,3-dimethylaminopropyl) carbodiimide (136 mg, 0.88 mmol), *N*-hydroxybenzotriazole (115 mg, 0.85 mmol), and triethylamine (0.20 mL). The reaction was stirred for 24 h at room temperature, then evaporated to yield a brown semi-solid, which was resuspended in chloroform and washed three times with water followed by brine. The organic layer was then evaporated and purified on a silica gel column by using 2% methanol in chloroform to give apo-**5** (545 g, 88%) as a pale-yellow semi-solid, which was a single peak in HPLC-MS (reversed-phase column; mobile phase gradient of 5% to 80% acetonitrile in 10 mM ammonium acetate over 10 min at 0.7 mL min^{-1}). ^1H NMR (300 MHz, $CDCl_3$): $\delta = 10.95$ (br s, 1H), 8.48 (d, $J = 5.1$ Hz, 4H), 7.56 (td, $J = 7.8$, 1.6 Hz, 4H), 7.45 (d, $J = 7.8$ Hz, 4H), 7.08 (m, 4H), 7.03 (s, 2H), 5.35 (d, $J = 9.0$ Hz, 1H), 4.63 (m, 1H), 3.80 (s, 8H), 3.72 (s, 4H), 3.15 (m, 1H), 2.95 (m, 1H), 2.84 (m, 4H), 1.86 (m, 4H), 1.33 (s, 9H), 0.95–1.30 (br s, 12H), 0.69–0.88 (m, 6H); ^{13}C NMR (75 MHz, $CDCl_3$): $\delta = 171.5$, 166.9, 159.2, 154.9, 148.8, 136.5, 130.4, 126.4, 124.0, 123.0, 121.9, 59.6, 54.7, 51.6, 47.8, 47.6, 46.2, 38.7, 31.5, 31.4, 31.2, 28.9, 28.3, 27.5, 26.6, 26.5, 26.3, 25.8, 22.5, 22.4, 14.0, 13.9; ES-MS: *m/z*: 872 $[M+H]^+$. Subsequent treatment with two molar equivalents of $Zn(NO_3)_2$ in aqueous methanol, followed by evaporation gave the zinc complex **5** in quantitative yield, which was used without further purification.

Zinc complex 6. The above-described procedure was used to make apo-**6** in 88% yield. ^1H NMR (300 MHz, $CDCl_3$): $\delta = 10.95$ (br s, 1H), 8.38 (d, $J = 5.1$ Hz, 4H), 7.49 (td, $J = 8.0$, 1.5 Hz, 4H), 7.36 (d, $J = 7.8$ Hz, 4H), 7.00 (m, 4H), 6.93 (s, 2H), 5.31 (d, $J = 9.2$ Hz, 1H), 4.58 (m, 1H), 3.72 (s, 8H), 3.64 (s, 4H), 3.07 (m, 1H), 2.88 (m, 1H), 2.75 (m, 4H), 1.69 (m, 4H), 1.27 (s, 9H), 0.95–1.26 (br s, 28H), 0.74 (t, $J = 7.2$ Hz, 6H); ^{13}C NMR (75 MHz, $CDCl_3$): $\delta = 171.4$, 166.9, 159.0, 154.8, 148.7, 136.5, 130.3, 126.2, 123.9, 122.9, 121.9, 59.5, 54.7, 47.9, 40.8, 31.7, 29.5, 29.4, 29.1, 29.0, 28.2, 27.5, 26.8, 26.5, 26.3, 22.5, 14.0; ES-MS: *m/z*: 984 $[M+H]^+$. Subsequent treatment with two molar equivalents of $Zn(NO_3)_2$ in aqueous methanol, followed by evaporation gave the zinc complex **6** which was used without further purification.

Vesicle preparation: All phospholipids were purchased from Avanti Polar Lipids (Alabaster, USA). An appropriate mixture of phospholipid was dried as a film in vacuo for 1 h. A stock solution of vesicles (10 mM phospholipid) was made by rehydration at room temperature with the appropriate buffer. Multilamellar vesicles were extruded to form unilamellar vesicles with a Basic Liposo-Fast device purchased from Avestin, Inc. (Ottawa, Canada). The vesicles were extruded 29 times through a 19 mm polycarbonate Nucleopore filter with 100 nm diameter pores.

Phospholipid translocation assay: The 7-nitrobenz-2-oxa-1,3-diazol-4-yl (NBD)-dithionite assay has been described previously.[17] Briefly, exo-labeled vesicles were prepared by slowly injecting a concentrated ethanolic solution of NBD-phospholipid into a stirred solution (35 mL) of vesicles (25 μM). An appropriate aliquot of the zinc complex in DMSO was added at 50 s, and translocation rates were determined from the subsequent change in %exo NBD-phospholipid over time. Every 15 min, a sample (3 mL) was removed and treated with 60 mM sodium dithionite solution and then Triton X-100 (final concentration of 0.5%). The %exo probe $= (F_i - F_f)/F_i$ where F_i and F_f are the NBD-phospholipid fluorescence intensities just prior to the addition of dithionite and Triton X-100, respectively. Excitation was set at 470 nm, and fluorescence emission was measured at 530 nm by using a 515 nm filter. The half-lives are the time periods to reach 80% exo probe and the values listed in Table 1 are the averages of three independent experiments.

Carboxyfluorescein leakage assay: Vesicles were prepared in the presence of rehydration buffer that contained 5 mM TES, 100 mM NaCl, 50 mM carboxyfluorescein (CF) buffer (pH 7.4). Unencapsulated CF was separated from the vesicles by filtration through a Sephadex-G50 column in TES buffer, or by overnight dialysis (12–14000 MWCO tubing from Sigma–Aldrich) and a buffer that contained 5 mM TES and 100 mM NaCl (pH 7.4). From this stock solution of vesicles, samples (3 mL) were assayed for leakage (ex: 495 nm, em: 520 nm) upon the addition of an aliquot of zinc complex in DMSO at 50 s and 20% (*v/v*) Triton X-100 (20 μL) at 750 s. The %CF release was calculated from Equation (1):

$$\%\ \text{CF release} = \frac{F_f - F_t}{F_f - F_i} \times 100 \quad (1)$$

Where F_i, F_t and F_f are the fluorescence intensities just prior to the additions of zinc complex and Triton X-100, and at the end of the experiment, respectively. All leakage experiments were reproduced at least three times.

Mammalian cell toxicity-MTT assay: Jurkat and LNCaP cells were cultured in 75 mL tissue culture flasks by using RPMI media with 10% fetal bovine serum (FBS). PC3 cells were cultured in 75 mL tissue culture flasks by using Ham's media with 10% FBS. All cells were grown at 37 °C, 5% CO_2 according to ATCC protocols.

MTT assays were run by using the Vybrant MTT Cell Proliferation Assay Kit (Invitrogen, V-13154). A mixture of cells (200 μL, approximately 5×10^4 cells per mL) in growth media were dispensed into each well of a 96-well plate and were allowed to grow for 48 h. An aliquot of zinc complex in DMSO was administered to each well with serial two-fold dilution. The wells were allowed to incubate for 24 h at 37 °C, then the growth medium was changed and a solution of 3-(4,5-dimethylthiazol-2-yl)-2,5-diphenyltetrazolium bromide (MTT; 10 μL of a 12 mM) in sterile PBS was added to each well. The cells were incubated at 37 °C for 4 h, then treated with an SDS·HCl solution (100 μL) to kill the cells and dissolve the formazan product. The SDS·HCl solution was prepared by adding 0.01 M HCl (10 mL) to SDS (1 g). The SDS·HCl per cell solution was then incubated for 24 h at 37 °C, after which the absorbance of the cells was read at 570 nm. Equation (2) was used to determine the percentage of living cells in each sample:

$$\%\ \text{living cells} = \frac{\text{Abs} - \text{Abs}_{\text{Neg}}}{\text{Abs}_{\text{Con}} - \text{Abs}_{\text{Neg}}} \times 100 \quad (2)$$

Where Abs is the absorbance of the test well, Abs_{Neg} is the absorbance of the negative control (no cells added) and Abs_{Con} is the absorbance of the positive control (10 μL vehicle added to live cells). The listed LD_{50} values are the average of three independent experiments.

Minimum inhibitory concentration: The minimum inhibitory concentration (MIC) for **1** is reported as the lowest serial two-fold dilution that prevented bacterial growth as outlined by the National Committee for Clinical Laboratory Standards (NCCLS). *E. coli* K12 cells were tested by using a bacterial load of 5×10^5 CFU mL^{-1}. Cells were grown at 37 °C in Luria Bertani (LB) Miller media (2 mL; 10 g L^{-1} peptone, 5 g L^{-1} yeast extract, and 10 g L^{-1} NaCl) that were twofold serially diluted with zinc complex **3**. *S. aureus* cells (listed in Table 1) were tested in similar fashion by using regular Mueller

Hinton II broth (300 g L^{-1} infusion from beef, 17.5 g L^{-1} casamino acids, 1.5 g L^{-1} bacto soluble starch) with the same microbial load. For *S. aureus*, the cells were grown in 96-well format by using total media (100 μL) in each well. For both organisms, the MIC was taken as the lowest concentration that inhibited growth after 24 h, as judged by visual turbidity. Each measurement of MIC was performed in triplicate.

Membrane depolarization studies: *S. aureus* cells were grown at 37 °C in Luria Bertani (LB) Miller media to mid-log phase, centrifuged, and the pellet washed once in 200 mM dextrose, 10 mM HEPES (pH 7.5) buffer. The resulting suspension was centrifuged again and resuspended to an OD_{600} of 0.6 in the same buffer. A stock solution of dye was made by dissolving 3,3-dipropylthiadicarbocyanine iodide ($DiSC_3(5)$; 1 mg) in DMSO (50 mL) in a foil-protected falcon tube. Fluorescence emission from $DiSC_3(5)$ was detected at 670 nm by using an excitation wavelength of 640 nm. A typical experiment began by adding dye solution (50 μL) to buffer (3 mL) in a disposable cuvette with continuous stirring throughout the experiment. Addition of the dye produced a sharp increase in fluorescence intensity, which quickly leveled off. This baseline was taken as the initial fluorescence value, I_o, for the data presented in Figure 5. Next, the *S. aureus* stock solution (300 μL) was added to give a final OD_{600} of 0.05. The fluorescence rapidly decreased and was allowed to stabilize and reach a new baseline with an I/I_o value of ~0.1. An aliquot of stock NaCl solution was added to give a 30 mM final concentration, followed by zinc complex **3** which produced a time-dependent increase in fluorescence intensity. The data ($n = 3$) were analyzed in Microsoft Excel 2003, and the average plus standard error of the mean (SEM) was plotted by using the GraphPad Prism V4.0.

Acknowledgements

This work was supported by the NIH (USA).

Keywords: antibiotics · fluorescent probes · membranes · phospholipids · zinc

[1] S.-K. Choi, *Synthetic Multivalent Molecules, Concepts and Biomedical Applications* Wiley, Hoboken, **2004**.
[2] a) *Making and Using Antibodies: A Practical Handbook* (Eds.: G. C. Howard, M. R. Kaser) CRC, Boca Raton, **2006**; b) S. J. Mather, *Mol. Biosyst.* **2007**, *3*, 30–35.
[3] *Handbook of Therapeutic Antibodies* (Ed.: S. Dübel), Wiley-VCH, Weinheim, **2007**.
[4] a) J. J. Khandare, T. Minko, *Crit. Rev. Ther. Drug Carriers* **2006**, *23*, 401–435; b) S. Jaracz, J. Chen, L. V. Kuznetsova, I. Ojima, *Bioorg. Med. Chem.* **2005**, *13*, 5043–5054.
[5] a) G. N. Tew, D. Clements, H. Tang, L. Arnt, R. W. Scott, *Biochim. Biophys. Acta Biomembr.* **2006**, *1758*, 1387–1392; b) R. F. Epand, M. A. Schmitt, S. H. Gellman, R. M. Epand, *Biochim. Biophys. Acta Biomembr.* **2006**, *1758*, 1343–1350; c) J. M. Rausch, J. R. Marks, W. C. Wimley, *Proc. Natl. Acad. Sci. USA* **2005**, *102*, 10511–10515; d) F. C. Odds, A. J. P. Brown, N. A. R. Gow, *Trends Microbiol.* **2003**, *11*, 272–279.
[6] W. M. Leevy, N. Serazin, B. D. Smith, *Drug Discovery Today: Dis. Models*, DOI: 10.1016/j.ddmod.2007.07.001.
[7] J. M. Boon, B. D. Smith, *Med. Res. Rev.* **2002**, *22*, 251–281.
[8] C. Ratledge, S. G. Wilkinson, *Microbial Lipids, Vol. 1*, Harcourt Brace Jovanovich, San Diego, **1988**.
[9] a) A. Giuliani, G. Pirri, S. F. Nicoletto, *Cent. Eur. J. Biol.* **2007**, *2*, 1–33; b) D. W. P. W. Löwik, J. C. M. van Hest, *Chem. Soc. Rev.* **2004**, *33*, 234–245; c) R. Jelinek, S. Kolusheva, *Curr. Protein Pept. Sci.* **2005**, *6*, 103–114.
[10] a) T. N. Lambert, B. D. Smith, *Coord. Chem. Rev.* **2003**, *240*, 129–141; b) C. Lakshmi, R. G. Hanshaw, B. D. Smith, *Tetrahedron* **2004**, *60*, 11307–11315; c) R. G. Hanshaw, B. D. Smith, *Bioorg. Med. Chem.* **2005**, *13*, 5035–5042.
[11] a) E. J. O'Neil, B. D. Smith, *Coord. Chem. Rev.* **2006**, *250*, 3068–3080; b) A. Ojida, M. Inoue, Y. Mito-oka, I. Hamachi, *J. Am. Chem. Soc.* **2003**, *125*, 10184–10185; c) A. Ojida, Y. Mito-oka, K. Sada, I. Hamachi, *J. Am. Chem. Soc.* **2004**, *126*, 2454–2463; d) S. Aoki, E. Kimura, *Chem. Rev.* **2004**, *104*, 769–788; e) A. Ojida, Y. Mito-oka, M. Inoue, I. Hamachi, *J. Am. Chem. Soc.* **2002**, *124*, 6256–6258; f) P. Molenveld, J. F. J. Engbersen, D. V. Reindoudt, *Chem. Soc. Rev.* **2000**, *29*, 75–86.
[12] W. M. Leevy, J. R. Johnson, C. Lakshmi, J. D. Morris, M. Marquez, B. D. Smith, *Chem. Commun.* **2006**, 1595–1597.
[13] a) W. M. Leevy, S. T. Gammon, H. Jiang, J. R. Johnson, D. J. Maxwell, E. N. Jackson, M. Marquez, D. Piwnica-Worms, B. D. Smith, *J. Am. Chem. Soc.* **2006**, *128*, 16476–16477; b) J. R. Johnson, N. Fu, E. Arunkumar, W. M. Leevy, S. T. Gammon, D. Piwnica-Worms, B. D. Smith, *Angew. Chem.* **2007**, *119*, 5624–5627; *Angew. Chem. Int. Ed.* **2007**, *46*, 5528–5531.
[14] a) M. S. Han, D. H. Kim, *Angew. Chem.* **2002**, *114*, 3963–3965; *Angew. Chem. Int. Ed.* **2002**, *41*, 3809–3811; b) D. H. Lee, J. H. Im, S. K. Son, Y. K. Chung, J. Hong, *J. Am. Chem. Soc.* **2003**, *125*, 7752–7753; c) D. H. Lee, S. Y. Kim, J. Hong, *Angew. Chem.* **2004**, *116*, 4881–4884; *Angew. Chem. Int. Ed.* **2004**, *43*, 4777–4780; d) R. G. Hanshaw, S. Hilkert, H. Jiang, B. D. Smith, *Tetrahedron Lett.* **2004**, *45*, 8721–8724.
[15] H. Jiang, E. J. O'Neil, K. M. DiVittorio, B. D. Smith, *Org. Lett.* **2005**, *7*, 3013–3017.
[16] a) K. Honda, S-H. Fujishima, A. Ojida, I. Hamachi, *ChemBioChem* **2007**, *8*, 1370–1372; b) A. Ojida, K. Honda, D. Shinmi, S. Kiyonaka, Y. Mori, I. Hamachi, *J. Am. Chem. Soc.* **2006**, *128*, 10452–10459; c) K. Honda, A. Ojida, I. Hamachi, *Chem. Commun.* **2006**, 4024–4026.
[17] Y. Sasaki, R. Shukla, B. D. Smith, *Org. Biomol. Chem.* **2004**, *2*, 214–219.
[18] The structure and stoichiometry of anion coordination to these zinc complexes will be described in a future publication.
[19] B. D. Smith, T. N. Lambert, *Chem. Commun.* **2003**, 2261–2268.
[20] a) A. P. Davis, D. N. Shephard, B. D. Smith, *Chem. Soc. Rev.* **2007**, *36*, 348–357; b) B. A. McNally, W. M. Leevy, B. D. Smith, *Supramol. Chem.* **2007**, *19*, 29–37.
[21] J. Gao, Y.-G. Liu, Y. Zhou, L. M. Boxer, F. R. Woolley, R. A. Zingaro, *ChemBioChem* **2007**, *8*, 332–340.
[22] N. W. Goehring, J. Beckwith, *Curr. Biol.* **2005**, *15*, R514–R526.
[23] M. G. Pinho, J. Errington, *FEMS Microbiol. Lett.* **2004**, *240*, 145–149.
[24] a) K. Tiyanont, T. Doan, M. B. Lazarus, X. Fang, D. Z. Rudner, S. Walker, *Proc. Natl. Acad. Sci. USA* **2006**, *103*, 11033–11038; b) E. Glukhov, M. Stark, L. L. Burrows, C. M. Deber, *J. Biol. Chem.* **2005**, *280*, 33960–33967; c) M. W. Disney, J. Zheng, T. M. Swager, P. H. Seeberger, *J. Am. Chem. Soc.* **2004**, *126*, 13343–13346.
[25] National Committee for Clinical Laboratory Standards, *Methods for Dilution Antimicrobial Susceptibility Tests for Bacteria that Grow Aerobically*, NCCLS, Wayne, Pennsylvania, **2000**, 5th ed., M7–A5.
[26] S. B. Al-Masaudi, M. J. Day, A. D. Russel, *J. Appl. Bacteriol.* **1988**, *65*, 329–337.
[27] M. H. Rayner, P. J. Sadler, *FEMS Microbiol. Lett.* **1990**, *71*, 253–258.
[28] M. Kruppa, B. Burkhard, *Chem. Rev.* **2006**, *106*, 3520–3560.
[29] L. Arnt, J. R. Rennie, S. Linser, R. Willumeit, G. N. Tew, *J. Phys. Chem. B* **2006**, *110*, 3527–3532.
[30] A. A. Gurtovenko, L. Vattulainen, *J. Am. Chem. Soc.* **2005**, *127*, 17570–17571.
[31] A. B. Zafar, R. C. Butler, D. J. Reese, L. A. Gaydos, P. A. Menonna, *Am. J. Infect. Control* **1995**, *23*, 200–208.
[32] M. T. E. Suller, A. D. Russell, *J. Antimicrob. Chemother.* **2000**, *46*, 11–18.
[33] S. Torelli, C. Belle, I. Gautier-Luneau, J. L. Pierre, E. Saint-Aman, J. M. Latour, L. Le Pape, D. Luneau, *Inorg. Chem.* **2000**, *39*, 3526–3536.

Received: August 23, 2007
Published online on December 12, 2007

